Plant Molecular Biology
https://doi.org/10.1007/s11103-022-01273-w

Regulatory mechanisms behind the phenotypic plasticity associated with *Setaria italica* water deficit tolerance

Vanessa Fuentes Suguiyama[1] · Jae Diana Paredes Rodriguez[1] · Tatiane Cristina Nicomedio dos Santos[1] · Bruno Silvestre Lira[2] · Luis Alejandro de Haro[3] · João Paulo Naldi Silva[1] · Eduardo Leite Borba[4] · Eduardo Purgatto[5] · Emerson Alves da Silva[6] · Nicolas Bellora[7] · Fernando Carrari[8,9] · Danilo da Cruz Centeno[1] · Luisa Fernanda Bermúdez[8,9] · Magdalena Rossi[2] · Nathalia de Setta[1]

Received: 20 December 2021 / Accepted: 11 April 2022

Abstract

Drought is one of the main environmental stresses that negatively impacts vegetative and reproductive yield. Water deficit responses are determined by the duration and intensity of the stress, which, together with plant genotype, will define the chances of plant survival. The metabolic adjustments in response to water deficit are complex and involve gene expression modulation regulated by DNA-binding proteins and epigenetic modifications. This last mechanism may also regulate the activity of transposable elements, which in turn impact the expression of nearby loci. *Setaria italica* plants submitted to five water deficit regimes were analyzed through a phenotypical approach, including growth, physiological, RNA-seq and sRNA-seq analyses. The results showed a progressive reduction in yield as a function of water deficit intensity associated with signaling pathway modulation and metabolic adjustments. We identified a group of loci that were consistently associated with drought responses, some of which were related to water deficit perception, signaling and regulation. Finally, an analysis of the transcriptome and sRNAome allowed us to identify genes putatively regulated by TE- and sRNA-related mechanisms and an intriguing positive correlation between transcript levels and sRNA accumulation in gene body regions. These findings shed light on the processes that allow *S. italica* to overcome drought and survive under water restrictive conditions.

Key message

Setaria italica cultivated under water deficit shows phenotypical plasticity associated with stress intensity, which is regulated, at least in part, by complex sRNA-dependent gene expression regulation mechanisms.

Keywords Monocots · SRNAs · Transcriptome · Plant metabolism · Transposable elements

✉ Nathalia de Setta
nathalia.setta@ufabc.edu.br

[1] Centro de Ciências Naturais e Humanas, Universidade Federal do ABC, São Bernardo do Campo, SP, Brazil

[2] Departamento de Botânica, Instituto de Biociências, Universidade de São Paulo, São Paulo, SP, Brazil

[3] Departament of Plant and Environmental Sciences, Weizmann Institute of Science, Rehovot, Israel

[4] Departamento de Botânica, Instituto de Ciências Biológicas, Universidade Federal de Minas Gerais, Belo Horizonte, MG, Brazil

[5] Departamento de Alimentos e Nutrição Experimental, Faculdade de Ciências Farmacêuticas, Universidade de São Paulo, São Paulo, SP, Brazil

[6] Instituto de Botânica da Secretaria do Meio Ambiente do Estado de São Paulo, São Paulo, SP, Brazil

[7] Institute of Nuclear Technologies for Health (Intecnus), National Scientific and Technical Research Council (CONICET), 8400 Bariloche, Argentina

[8] Instituto de Agrobiotecnología Y Biología Molecular (IABIMO), CICVYA, INTA-CONICET, Hurlingham, Argentina

[9] Cátedra de Genética, Facultad de Agronomía, Universidad de Buenos Aires, Buenos Aires, Argentina

Published online: 07 May 2022

Introduction

Drought is one of the most important abiotic stresses impacting vegetative and reproductive crop growth (Lata et al. 2010; Basu et al. 2016). In general, the biological responses to an environmental stress are determined by its duration, intensity and the plant genotype (Chaves et al. 2003; Basu et al. 2016; Laxa et al. 2019). In grasses, it has been reported that drought stress up-regulates the expression of a wide range of osmoprotective molecules to avoid damage by reactive oxygen species (ROS) (Laxa et al. 2019), decreases photosynthesis (Fracasso et al. 2016), impacts carbohydrate and amino acid metabolism to provide osmotically active compounds, as well as signaling molecules (Qi et al. 2013), alters flowering time and morphology (Su et al. 2013; Kang and Futakuchi 2019), and reduces growth rate and biomass production (Sun et al. 2016).

Drought-tolerant plants can deal with water stress, thus avoiding permanent damage and ensuring vegetative and reproductive growth by means of phenotypic plasticity (Nicotra et al. 2010; Basu et al. 2016). Plastic phenotypes are mainly determined by gene expression reprogramming regulated at different levels (Sudan et al. 2018), including transcriptional regulation mediated by transcription factors (TFs) and epigenetic modifications (Liu and Stewart 2016; Brkljacic and Grotewold 2017; Hoang et al. 2017). In plants, epigenetic regulation includes three interconnected mechanisms: DNA methylation, posttranslational histone modification and RNA interference (RNAi) (Sudan et al. 2018). RNAi is mediated by small RNAs (sRNAs) that, in turn, drive transcriptional (TGS) and posttranscriptional (PTGS) gene silencing (Hung and Slotkin 2021). It is known that TGS is mediated by 24 nt and 21–22 nt small interfering RNAs (siRNAs) through canonical and non-canonical RNA-directed DNA methylation (RdDM), respectively (Hung and Slotkin 2021). Additionally, 21–22 nt sRNAs participate in PTGS pathways (Cuerda-Gil and Slotkin 2016). RNAi functions as a defense against transposable elements (TEs) and virus activity and, in plants, contributes to development and stress response (Chang et al. 2020; Hung and Slotkin 2021), which are associated with gene expression modulation of TEs and other repeats near loci (Lisch 2009; Quadrana et al. 2014; Matzke and Mosher 2014).

The model C4 grass species *Setaria italica* (L.) P. Beauv. is an annual plant domesticated from *Setaria viridis* (Doust et al. 2009; Bennetzen et al. 2012). During the domestication process, *S. italica* was gradually adapted to tolerate arid and semiarid climates (Doust et al. 2009). When grown under drought conditions, *S. italica* shows declined photosynthesis parameters that result in reduction of growth, grain yield and biomass (Xu et al. 2006; Tang et al. 2017; Nematpour et al. 2019). Moreover, drought promotes the remodeling of *S. italica* metabolic pathways, such as lipids, amino acids, phytohormones and carbohydrates, together with the up-regulation of osmoprotectant and stress-related genes (Qi et al. 2013; Tang et al. 2017). These metabolic adjustments were combined with changes in the expression of drought-related TFs, such as those of AP2/EREF, bZIP, MYB, NAC and WRKY families (Qi et al. 2013; Tang et al. 2017), and differential accumulation of 24-nt siRNA in flanking regions of drought-responsive genes (Qi et al. 2013).

In this context, studies approaching plant water deficit responses on a comprehensive scale, integrating yield, physiological, transcriptome and sRNAome analyses are indispensable to improve the knowledge about the mechanisms that allow plant survival under water deficit. In addition, although the influence of TEs on abiotic stress responses has been demonstrated, the underlying molecular mechanisms remain poorly understood. Here, we show that *S. italica* cultivated under distinct watering regimes displayed a positive association between growth parameters and water availability. Changes in vegetative and reproductive development were accompanied by physiological, biochemical, and gene expression modulation. We were able to catalogue 'stress-related' and 'severe stress-related' differentially expressed genes (DEGs), including several loci putatively involved in the water deficit signaling response. Finally, we propose that complex sRNA-dependent gene expression regulation mechanisms participate in the *S. italica* water stress response.

Materials and methods

Plant material and water deficit experimental design

The *S. italica* Yugu1 plants were grown in a chamber under an air temperature of 26 ± 2 ºC, 50–60% relative humidity, 16 h photoperiod and photosynthetic photon flux density (PPDF) of 400—500 µmol m^{-2} s^{-1} until seed harvesting. Seeds from an individual plant were sown in 50 ml pots (one seed per pot) containing a 3:1 mixture of commercial substrate (Tropstrato HT, Viva Verde, Brazil) and expanded vermiculite under daily watering. Later, fifty 14-day-old seedlings were transplanted to pots containing 5 L of 3:1 mix of nutrient soil and expanded vermiculite supplemented with 1 g l^{-1} of NPK 10:10:10 and 4 g l^{-1} dolomite limestone ($MgCO_3 + CaCO_3$) and maintained at the same growth chamber conditions during the experiment. Right after seedling transfer, substrate was brought to field capacity. Then, we determined the mean evapotranspiration volume during the first 48 h of experiment based on gravimetric

measurements. The mean volume of evapotranspiration was 200 ± 3 ml. Based on this volume, five watering treatments, comprising 10 biological replicates each, were applied: 100% (200 ml every 48 h), 60% (120 ml every 48 h), 30% (60 ml every 48 h), 5% (10 ml every 48 h) and 0% (no watering). Every two weeks, before watering, the soil water content (SWC) was estimated by time domain reflectometry (TDR) using the sensor ML3 ThetaProbe of the Moisture Meter type HH2 (Delta-T Devices), calibrated to organic soil. The water stress experiment was conducted from 15th August 2016 to 9th March 2017. After 38 days of treatment, when the SWC of the 0% treatment was close to zero and plants were in the leaf development stage of phenological BBCH-scale (Zadoks et al. 1974), the 9th and 11th leaves from the base were harvested. Leaf material was immediately frozen in liquid nitrogen and stored at − 80 °C for further molecular analyzes, or immediately used to estimate the foliar relative water content (RWC).

Water status and gas exchange parameters

The relative water content (RWC) was estimated using two segments of the midpoint of the 9th leaf blade for each plant using the equation RWC (%) = (FW-DW/TW-DW) × 100, where FW is the fresh weight, estimated immediately after leaf harvest; TW is the turgid weight, estimated after 96 h of immersion in distilled water; and DW is the dry weight, estimated 96 h after incubation at 70 °C (Weatherley 1950).

Instantaneous measurements of net carbon assimilation rates (A, µmol CO_2 m^{-2} s^{-1}), transpiration (E, mol m^{-2} s^{-1}) and stomatal conductance (g_s, mol m^{-2} s^{-1}) were performed in the 4th or 5th leaf blade from the apex using a portable infrared gas analyzer (IRGA, LCpro-SP, ADC BioScientific) under ambient CO_2 concentration (~ 420 ppm) and light saturated irradiance of 1,200 µmol photons m^{-2} s^{-1}. The measurements were carried out 38, 42, 51, 72 and 105 days after the beginning of watering treatments, between 11:00 am and 3:00 pm, in five plants from each treatment. The instantaneous water-use efficiency (WUEi) was calculated using the A/E ratio.

Vegetative and reproductive growth parameters

Vegetative plant growth was estimated by plant height (from the stem base to the apical meristem), number of expanded leaves, relative foliar area (length of midrib x width of the middle part of the even leaves counted from the base), number of nodes and shoot biomass. These parameters were measured every two weeks until the aerial part of the plant was fully dry. Panicles were harvested at physiological maturity, and reproductive parameters analyzed included panicle emergence time (days after sowing), panicle weight, panicle length, panicle width and estimate of seed number per panicle. For the latter, the panicles were divided into 10 transversal fragments, and the number of seeds in the middle and tip fragments was counted. The total number of seeds per panicle was calculated according to the following equation: number of seeds = (seeds in the upper tip + seeds in the bottom tip + seeds in the middle fragment)/0.3. The reproductive traits of the plants from the 5% and 0% treatments were considered zero, as they did not produce panicles.

Carbohydrate quantification

Sugar extraction was carried out using 20 mg of dry leaf mass from three biological replicates per treatment, as described previously (Suguiyama et al. 2014), with modifications. Briefly, soluble sugars were extracted eight times with 1.5 ml of 80% ethanol for 15 min at 80 ºC. The supernatants were recovered by centrifugation (5000 g, 5 min). One mililiter of the total extract was evaporated under vacuum, resuspended in 1 ml of ultrapure water, and filtered through a 0.22 µm membrane. Glucose, fructose, sucrose and raffinose were quantified by high-performance anion exchange chromatography with pulsed amperometric detection (HPAEC-PAD, Dionex) using a Carbopac PA1 column (250 × 4 mm, 5 µm particle size, Dionex) in an isocratic run with 18 mM NaOH as the mobile phase. The residues from sugar extraction were dried and starch content was estimated (Suguiyama et al. 2014).

Statistical analyses for physiological and growth parameters, and carbohydrate quantification

Dataset normality of independent parameters was verified by the Shapiro-Wilks modified test ($P < 0.05$). The results were compared using ANOVA (Tukey's test, $P < 0.05$) or Kruskal–Wallis test ($P \leq 0.05$), according to the normality test as indicated in the figure and table legends. Parameters collected throughout the experiment were compared using repeated measures ANOVA (Hotelling's test, $P < 0.05$). Analyses were performed using the statistical package InfoStat (https://www.infostat.com.ar/index.php). Principal component analysis (PCA) was carried out using all the vegetative and reproductive growth parameters and the PAST software (Hammer et al. 2001).

RNA and sRNA sequencing

Total RNA was extracted from 100 mg of frozen grinded leaves using TRIzol reagent (Invitrogen), and the residual genomic DNA was removed using the Turbo DNA-free kit (Thermo Fisher Scientific), according to the manufacturer's instructions. The RNA samples were spectrophotometrically quantified using the BioDrop Touch Duo (BioDrop). The integrity of the total RNA was further confirmed by

1.0% (w/v) agarose gel electrophoresis and by automated electrophoresis using a Bioanalyzer 2100 (Agilent Technologies) and Eukaryote Total RNA Pico Series II LabChip Kit. RNA samples with an RNA integrity number ≥ 6 were further sequenced. We sequenced RNA-seq and sRNA-seq Illumina libraries from two technical replicates of 100%, 30% and 0% treatments, each one consisting of a pool of RNA samples from two different plants, in a total of four plants per treatment. The six samples were used for both 100 bp paired-end read RNA sequencing (RNA-seq) and 50 bp single-end read sRNA sequencing (sRNA-seq) using the Hiseq4000 platform (Illumina), according to Illumina's protocol, at the Beijing Genomics Institute (BGI, China). RNA-seq samples were named 100%-1, 100%-2, 30%-1, 30%-2, 0%-1 and 0%-2. sRNA-seq samples were named 100%-1 s, 100%-2 s, 30%-1 s, 30%-2 s, 0%-1 s and 0%-2 s.

RNA-seq, differentially expressed gene identification and functional category enrichment analyses

Raw RNA-seq reads were trimmed for adaptors and poor quality bases using Trimmomatic v.0.32 (Bolger et al. 2014) and the following parameters: ILLUMINACLIP:TruSeq3-PE.fa:2:30:10, LEADING:3, TRAILING:3, SLIDINGWINDOW:4:20 and MINLEN:50. Reads that reached the quality scores Q ≥ 33 were indexed and aligned to the *S. italica* v2.2 reference genome (Bennetzen et al. 2012) available on Phytozome (http://phytozome.jgi.doe.gov) using GMAP and GSNAP v.2017-08-15 (Wu et al. 2016), allowing 5 mismatches per read (-m 5) and searching to detect splicing (-N 1). Counting of the number of reads mapped against the CDS (coding sequence) was performed using htseq-count v.0.8.0 (Anders et al. 2015). Differentially expressed genes (DEG) identification were performed for the comparisons of 100% versus 30% (100% × 30%), 100% versus 0% (100% × 0%) and 30% versus 0% (30% × 0%) treatments. Gene expression was estimated by negative binominal distribution using two computational tools, EdgeR v.3.18.1 (Robinson et al. 2010) and DESeq2 v.1.16.1 (Love et al. 2014) of the Bioconductor R package (Gentleman et al. 2004) to improve the reliability of the RNA-seq data analysis. Genes were considered differentially expressed if they met the criteria of FDR-adjusted P ≤ 0.05 for both methods and the screening cut-off of $\log_2$-ratio ≤ − 1.0 or ≥ 1.0. Gene expression multidimensional analysis (MA) plots and principal component analysis (PCA) were generated using EdgeR v.3.18.1, with default parameters. DEGs of 100% × 30%, 100% × 0% and 30% × 0% comparisons were categorized using the MapMan platform (Usadel et al. 2009), according to the functional BINs from the Mercator 3.6 annotation system (Lohse et al. 2014), with default parameters.

Setaria italica water deficit signaling pathway reconstruction

The identification of *S. italica* loci involved in water deficit signaling was performed based on the *Arabidopsis thaliana* water deficit signaling literature. We searched for putative *A. thaliana*/*S. italica* homologous gene pairs using PhyloGenes (www.phylogenes.org/) and the Protein Homologs tool available in the Phytozome database (phytozome.jgi.doe.gov/pz/portal.html#). Gene model accession codes and sequences of *A. thaliana* loci were retrieved from TAIR (www.arabidopsis.org/index.jsp). The results were validated using gene annotation from the *S. italica* v2.2 reference genome (Bennetzen et al. 2012) and MapMan functional annotation (Usadel et al. 2009). The schematic diagram was designed using the BioRender.com tool.

Quantitative RT-qPCR validation

DEGs were validated by reverse transcription followed by quantitative PCR (RT-qPCR) in a 7500 real-time PCR system (Applied Biosystems) using the same biological samples used in the RNA-seq. The reactions were performed in a final volume of 14 µl with 2 × SYBR Green Master Mix reagent (Applied Biosystem) and 200 nM of each primer (Table S1). Absolute fluorescence data was used to calculate Ct values and primer efficiency using LinRegPCR software (Ruijter et al. 2009). Expression values were normalized using the *CULLIN* reference gene as previously proposed (Lambret-Frotté et al. 2015). A permutation test, lacking the sample distribution assumption (Pfaffl et al. 2002), was applied to detect differences (P ≤ 0.05) in expression ratios using fgStatistics software package version 17/05/2012 (https://sites.google.com/site/fgstatistics).

sRNA-seq and TE data analyses

Raw sRNA-seq reads were trimmed for adaptors and poor quality bases using Trimmomatic tool v.0.32 and the following parameters: ILLUMINACLIP:TruSeq3-SE:2:30:10, LEADING:3, TRAILING:3, SLIDINGWINDOW:4:20 and MINLEN:18 (Bolger et al. 2014). Reads with a Q ≥ 33 and 20–24 nt long were mapped against the *S. italica* v2.2 genome (Bennetzen et al. 2012) using ShortStack version 3.4 (Axtell 2013), with default parameters and no mismatches allowed. Small RNA accumulation was evaluated in gene body regions (CDSs, introns and UTR sequences), regulatory regions (2 kb upstream of the transcription initiation site) and TEs. Loci with count numbers smaller than two per million were removed. Count values were normalized according to the library size factors. Statistical analyses were performed with EdgeR v.3.18.1 using a genewise negative binomial generalized linear model with the quasi-likelihood

test and a cut-off of $P \leq 0.05$ and log2-ratio ≤ -1.0 or ≥ 1.0. Loci with significant differences in sRNA accumulation were considered sRNAs differentially accumulating loci (sRDALs). TEs were de novo annotated using the RepeatMasker tool (www.repeatmasker.org), with default parameters, and two reference databases: Repabse Viridiplantae (www.girinst.org/repbase/) and a *S. italica* LTR retrotransposon database (Suguiyama et al. 2019).

Results

The performance of plants growing under water deficit conditions

To study *S. italica* phenotypic responses to different levels of soil water content, 14-day-old seedlings were transferred to 5 L pots and grown in a chamber under controlled air temperature, relative humidity, and photoperiod until senescence. Right after seedling transplantation, pots were watered to bring the substrate to field capacity and then, five watering regimes supplied 200 ml (100% treatment), 120 ml (60% treatment), 60 ml (30% treatment), 10 ml (5% treatment), and none (0%) of water every 48 h (see Material and Methods). The soil water content (SWC) measurements showed a progressive decrease in the water availability during the experiment for all treatments (Supplementary Fig. 1). Moreover, except for the 5% and 0% treatments, the SWC was different between treatments, indicating that the experimental design was efficient in providing a decreasing gradient of water availability. On the 38th day after the beginning of the treatment, when the SWC of the 0% treatment was close to zero, the leaves for further physiological, biochemical and transcriptome/sRNA analyses were harvested.

During the first 24 days of treatment, the plants showed similar vegetative growth parameters for all five treatments (Fig. 1a–c). Beyond this point, plants from the 5% and 0% treatments displayed the lowest values for all growth parameters evaluated, followed by the 30% and then, 100% and 60% treatment plants. For example, plants in the 0% treatment had a decrease of approximately 90% in shoot biomass and 80% in height compared to the 100% treatment plants (Table 1). All plants in the 5% and 0% treatments perished 72 days after the beginning of water deficit and were not able to produce panicles. On the other hand, all 100% and 60% treatment plants produced mature panicles, completing their life cycle after 182 days of treatment. Finally, 30% treatment plants had a developmental delay, flowering 20 days later than the 100% and 60% treatment plants (Table 1), and perished after 206 days of water deficit. Additionally, 30% treatment plants had smaller panicles and fewer seeds than plants of the 100% and 60% treatments (Table 1).

Principal component analysis (PCA) was used to evaluate the similarity of the vegetative and reproductive growth responses between treatments (Fig. 1d). PC1 explained almost 90% of the variance among the samples. The clustering pattern revealed that plants from the 100% and 60% treatments were similar, indicating that the 60% watering regime was not restrictive enough to induce differences from the 100% treatment. The 30% treatment plants showed an intermediate vegetative and reproductive profile, while plants from the 5% and 0% treatments clustered together.

The relative water content (RWC) of leaves after 38 days of treatment was $92.96\% \pm 0.76$, $91.04\% \pm 0.87$ and $87.77\% \pm 2.02$ for plants from 100%, 60% and 30% water regimes, respectively. These percentages were not significantly different among each other but were higher than the RWC of 5% ($84.07\% \pm 1.28$) and 0% ($84.91\% \pm 1.31$) treatment plants ($P < 0.001$). Gas exchange parameters were different among treatments, displaying a positive association with water availability (Fig. 1e–g). Interestingly, on the 38th day of treatment, 5% and 0% treatment plants showed higher net carbon assimilation (*A*) rate than the other treatments. Similarly, the transpiration (*E*) was also higher for the 0% treatment plants than or the other treatments on the 38th day (Supplementary Table 2). Regarding the instantaneous water-use efficiency (WUEi), it is worth highlighting that until the 42nd day of treatment, the plants from the lowest water availability treatments had the highest WUEi values, which further inverted (Fig. 1h; Supplementary Table 2). To obtain an overview of the carbon metabolism of *S. italica* grown under water deficit regimes, we performed soluble sugar and starch quantification of leaves harvested after 38 days of treatment. We were not able to identify differences in the levels of glucose, fructose, sucrose, raffinose and starch between treatments (Supplementary Table 3).

Setaria italica water deficit-related transcriptome

We further analyzed the *S. italica* gene expression profile in leaves from 100%, 30% and 0% treatment plants, i.e., the treatments that induced the most contrasting vegetative and reproductive growth parameters. Foliar tissues of plants submitted to 38 days of water deficit treatment were sequenced using Illumina platform (see Material and Methods for more details). We obtained approximately 40 million 100 base paired-end reads per library, and approximately 99% of those were properly mapped against the *S. italica* genome (Supplementary Table 4). On average, 18 million reads per sample aligned against 26,429 (76.42%) predicted CDSs of the *S. italica* genome.

MA plots from differential expression analyses showed that the three treatments had differences in the gene expression profiles, mainly for the $100\% \times 30\%$ and $100\% \times 0\%$ comparisons (Supplementary Fig. 2a-b). The PCA analyses

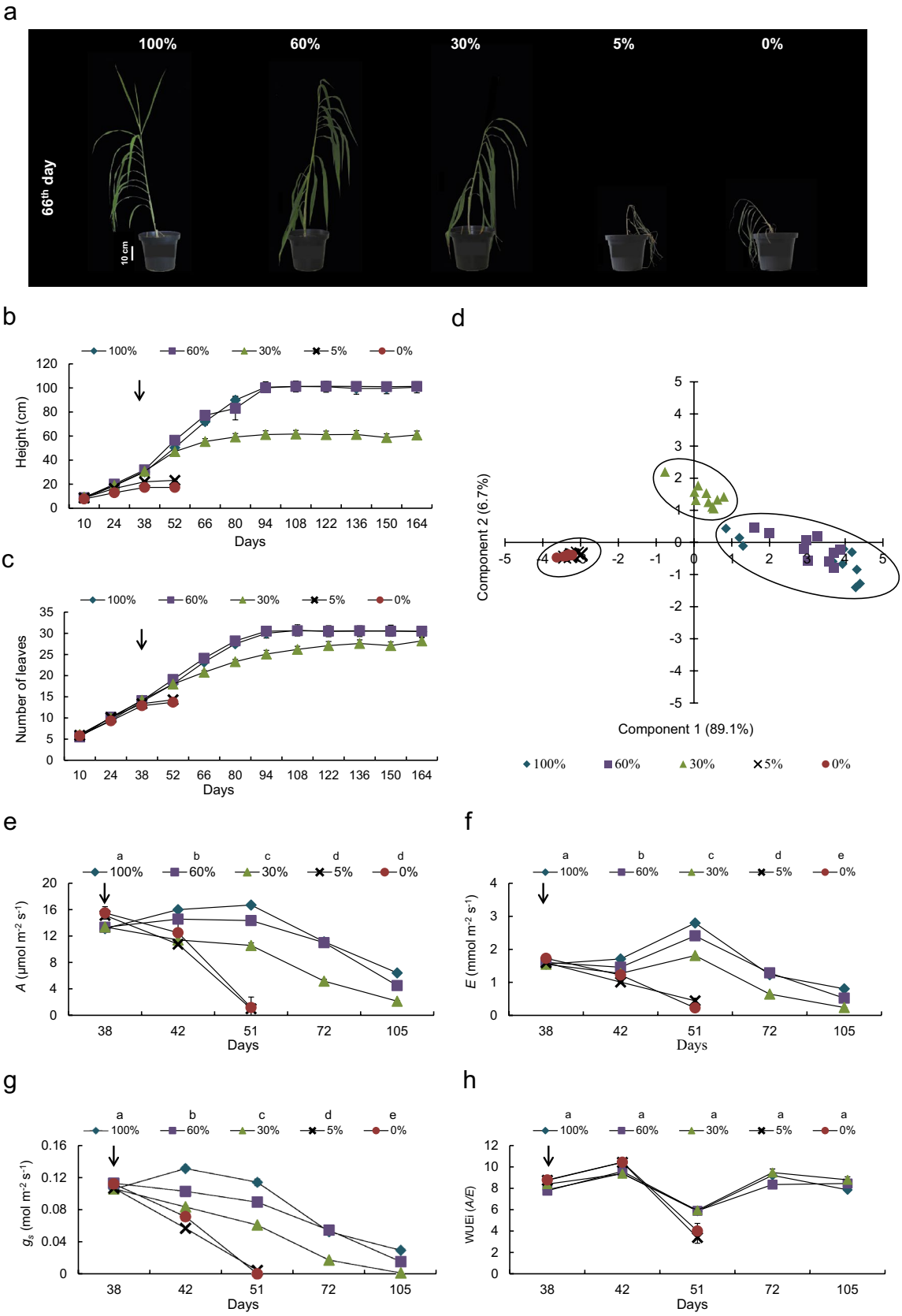
a
100%
60%
30%
5%
0%
66th day
10 cm
b
Height (cm)
Days
c
Number of leaves
Days
d
Component 2 (6.7%)
Component 1 (89.1%)
e
A (μmol m-2 s-1)
Days
f
E (mmol m-2 s-1)
Days
g
gs (mol m-2 s-1)
Days
h
WUEi (A/E)
Days

◂**Fig. 1** *Setaria italica* performance is impacted by the water deficit treatment. **a** Illustrative picture of *S. italica* plants after 66 days of water stress treatments (n = 10 biological replicates per treatment). **b** Height (mean ± SE) and **c** number of leaves (mean ± SE). **d** Principal component analysis (PCA) of vegetative and reproductive parameters. Each data point represents one independent biological replicate. Open ovals indicate different treatment clustering. **e** Carbon assimilation rate (*A*, mean ± SE), **f** transpiration (*E*, mean ± SE), **g** stomatal conductance (g_S, mean ± SE), and **h** instantaneous water efficiency use (WUEi, mean ± SE). Different letters above the legend represent the repeated measures ANOVA (Hotelling's test, $P \leq 0.05$) results among treatments. The values of gas exchange analysis, as well as the ANOVA comparisons of each day, are available in Supplementary Table 2. Fifty-two days after the beginning of the experiment, more than 50% of plants from the5% and 0% treatments had died. The arrows indicate the leaf harvest day for RNA- and sRNA-seq analyses

evidenced reproducibility between replicates and indicated that the normalized differences in expression patterns were the major source of dataset variation (Supplementary Fig. 2c-d). Approximately 90% of the DEGs identified by DESeq2 and EdgeR tools were common, and those 1,947 were used for further analyses. Thirty-two DEGs were common to all three comparisons, and 363, 120 and 17 DEGs were shared by two comparisons (Fig. 2a; Supplementary Table 5). RT-qPCR was used to validate the RNA-seq experiment. Nine DEGs had their relative transcription ratios evaluated for the 100% × 30%, 100% × 0% and 30% × 0% treatment comparisons using RT-qPCR and the results were further compared with the mean number of reads sequenced in the RNA-seq experiment. RNA-seq and RT-qPCR results were highly correlated ($R^2 = 0.9258$) validating more than 85% of the comparisons (Supplementary Figs. 3 and 4).

To MapMan categories, 1,346 DEGs were mapped, identifying 27, 33 and 24 main BINs for 100% × 30%, 100 × 0%, and 30% × 0% comparisons, respectively (Supplementary Table 6). The three comparisons had similar BIN mapping profiles. As expected for the most contrasting phenotypes, the 100% × 0% comparison showed the highest number of mapped DEGs, followed by the 100% × 30% and 30% × 0% comparisons (Fig. 2b). The BINs with the highest number of DEGs mapped were signaling, protein, RNA, transport, stress, secondary metabolism, and hormone metabolism. Additionally, the subcategories with the most DEGs mapped were signaling/receptor kinases (BIN 30.2, 173 DEGs), RNA/regulation of transcription (BIN 27.3; 156 DEGs), protein/degradation (BIN 29.5; 115 DEGs), protein/posttranslational modification (BIN 29.4; 64 DEGs), and secondary metabolism/flavonoids (BIN 16.8; 55 DEGs) (Supplementary Table 6).

Differentially expressed genes (DEGs) along a water deficit gradient unravel water stress-related signaling pathway

We further mined all the DEGs (Fig. 2) for loci with water stress signaling pathway-related products (Takahashi et al. 2018; Konopka-Postupolska and Dobrowolska 2020). The experimental design and transcriptome data allowed the identification of 27 genes putatively involved from ABA biosynthesis to water stress mitigation (Fig. 3; Supplementary Table 7). Two loci encoding the ABA biosynthetic enzyme 9-CIS-EPOXYCAROTENOID DIOXYGENASE (NCED) were up-regulated in both the 30% and 0% treatments. DEGs homologous to receptors and kinases involved in ABA/dehydration perception were also up-regulated: a pair of *PYRABACTIN RESISTANCE 1/PYR1-LIKE/REGULATORY COMPONENT OF ABA RECEPTORS* (*PYR/PYL/RCAR*), five *PROTEIN PHOSPHATASE 2C* (*PP2C*) and two *SNF1-RELATED KINASE 2 FAMILY 2* (*SnRK2*) homologs. Two homologs to the *A. thaliana* water deficit responsive *MITOGEN ACTIVATED PROTEIN KINASE 3* (*MAPK3*) and *MITOGEN ACTIVATED PROTEIN KINASE 9/12* (*MAPK9/12*) genes were up-regulated in both the 30% and 0% treatments. DEGs encoding putative Ca^{2+}-binding proteins capable of responding to or decoding dehydration signals were differentially expressed in water deficit treatments: three *CALCIUM-DEPENDENT PROTEIN KINASES* (*CPDKs*), two *CALMODULIN-LIKE PROTEINS* (*CMLs*) and two *CALCINEURIN B-LIKE PROTEIN KINASES* (*CIPKs*).

The ABA-PYR/PYL/RCAR-PP2C-SnRK2 module, MAPK and calcium-dependent pathways activate several drought downstream effectors, such as stomatal closure-related ion channels, ROS burst proteins, and transcription factors. *Setaria italica* loci homologous to these protein-encoding genes were also differentially expressed (Fig. 3; Supplementary Table 7). A putative *SLOW ANION CHANNEL 1* (*SLAC1*) and a *NADPH OXIDASE RESPIRATORY BURST OXIDASE HOMOLOG D* (*RBOHD*) loci were up-regulated. Finally, water stress-related transcription factors were also differentially expressed under water deficit. Two putative *ABRE-BINDING FACTOR 3* (*ABF3*) and a putative *DRE-BINDING PROTEIN 2A* (*DREB2A*) loci were up-regulated in the 0% treatment. Moreover, two putative WRKY18/40/60 were highly down-regulated in the 30% and 0% treatments.

Table 1 Vegetative and reproductive parameters (mean ± SE) of *S. italica* cultivated under five different watering treatments

Trait	100%	60%	30%	5%	0%
Maximum height* (cm)	100.6 ± 4.6^{a}	101.3 ± 3.1^{a}	61.0 ± 3.3^{b}	23.2 ± 0.8^{c}	17.3 ± 0.5^{c}
Total number of leaves*	30.4 ± 1.2^{a}	30.5 ± 0.5^{a}	28.2 ± 0.8^{a}	14.3 ± 0.3^{b}	13.7 ± 0.3^{b}
Estimative of foliar area* (cm^2)	3050.0 ± 223.4^{a}	3010.9 ± 116.2^{a}	1911.4 ± 85.3^{b}	630.6 ± 33.6^{c}	474.9 ± 23.9^{c}
Number of nodes*	17.5 ± 0.4^{a}	19.4 ± 0.5^{a}	13.2 ± 0.6^{b}	7.2 ± 0.5^{c}	6.4 ± 0.3^{c}
Shoot biomass** (g)	15.4 ± 1.7^{a}	12.8 ± 0.7^{a}	7.7 ± 0.6^{b}	2.3 ± 0.1^{c}	1.7 ± 0.1^{c}
Emergence of panicle (DAS)	97.1 ± 4.5^{a}	104.9 ± 3.5^{a}	124.6 ± 6.5^{b}	–	–
Weight of panicle** (g)	14.8 ± 2.2^{a}	12.5 ± 1.4^{a}	2.6 ± 0.3^{b}	–	–
Panicle length** (cm)	20.4 ± 1.4^{a}	18.6 ± 0.9^{a}	9.5 ± 0.5^{b}	–	–
Panicle width** (cm)	2.1 ± 0.2^{a}	2.1 ± 0.2^{a}	1.5 ± 0.0^{b}	–	–
Estimative of seeds numbers**	6777.3 ± 728.4^{a}	6736.2 ± 431.7^{a}	972.5 ± 245.4^{b}	–	–

Different superscript letters (a, b and c) indicate statistically significant differences as calculated by ANOVA (Tukey's test, $P \leq 0.05$) for ten biological replicates

DAS: days after sowing

*Parameters measured every two weeks until leaves were fully dry

**Parameters measured on the panicle harvest day

Stress-related and severe stress-related DEGs evidenced pathways consistently impacted by water deficit

To better understand the gene expression modulation that underlies water deficit responses in *S. italica*, we focused the analysis on the hereafter named Stress-Related (SR) and Severe Stress-Related (SSR) DEGs (Fig. 2a; Supplementary Table 5). These genes were the most robust and stringent representatives of the water deficit expression profile. SR DEGs were those differentially expressed in both the 30% and 0% treatments compared to the 100% treatment (363 genes), as well as those genes differentially expressed in the three comparisons (32 genes). The SSR DEGs, on the other hand, were those differentially expressed only in the most severe water deficit treatment, being shared between the 100% × 0% and 30% × 0% comparisons (120 genes). From the 278 SR and 70 SSR MapMan annotated genes, we focused on those 179 categorized as stress-related BINs according to MapMan, which could be divided into three groups: signal perception and transduction, downstream regulators, and defense genes (Fig. 4; Supplementary Table 6). Several water deficit-related genes were down-regulated, including genes in auxin, salicylic acid, signaling/receptor kinases, WRKY and MYB transcription factors and secondary metabolites BINs. On the other hand, ABA and AP/EREPB transcription factor BINs were mostly up-regulated. It is worth noting the mapping of several DEGs in the proteolysis, redox state, and peroxidase BINs. Interestingly, 48% of the genes included in the water stress signaling pathway (Fig. 3) are SR genes, including two WRKY transcription factors, two MAPK kinases, RBOHD, and four from five PP2C kinases. This result pinpoints 13 *S. italica* loci as strongly associated with the canonical drought stress response pathway.

sRNA-mediated gene expression regulation in response to water stress

The role of sRNAs in the regulation of gene expression in *S. italica* under water deficit was addressed by sRNA-seq using the same samples used in the RNA-seq experiment. We sequenced from 33 to 40 million reads per replicate, which were mapped against three genomic contexts: gene bodies (CDSs, introns and UTR sequences), regulatory regions (2 kb upstream transcription initiation site) and TE insertions (Supplementary Table 8). Regarding the length of sRNA reads, gene body regions were enriched for 21–22 nt sRNAs, and regulatory and TE regions were enriched for 24 nt sRNAs (Fig. 5). The 100% × 0% comparison displayed a higher number of sRNA differential accumulating loci (sRDALs) in the three genomic contexts, followed by the 30% × 0% and 100% × 30% comparisons (Fig. 6a; Supplementary Table 9). Most of the sRDALs were annotated as TE insertions, followed by gene body and regulatory regions. The sRDALs were mostly from protein, RNA, signaling, transport and stress MapMan functional categories (Fig. 6b; Supplementary Table 10).

We further focused our analysis of sRNAs on the 515 SR and SSR DEGs (Fig. 2a) and evaluated whether they were sRDALs, which might indicate epigenetic regulation of water stress-responsive genes. Almost half of the SR and SSR DEGs (239) were also sRDALs, and for most of them (216), the sRNA clusters mapped to the gene body regions (Supplementary Table 11). Additionally, six and 14 loci

showed sRNA differential accumulation on TE sequences (sRDATs) located in the gene body and regulatory regions, respectively. These sRDAT loci code for proteins annotated in several MapMan BINs, including RNA/regulation of transcription, signaling, transport, minor CHO metabolism and hormone metabolism (Supplementary Tables 6 and 11).

A clear positive correlation was observed between the expression of the DEGs and the sRNA accumulation patterns in gene body regions, which was not observed for the regulatory regions (Fig. 7). This agrees with the fact that up-regulated sRDALs mapped preferentially against gene body regions of transcripts with high counts per million (CPM) levels, a pattern that was not observed for regulatory regions (Supplementary Fig. 5). The sRDAL mapping profiles were analyzed in detail and a clear example of the positive correlation between expression and gene body sRNA accumulation is the case of the *O-METHYLTRANSFERASE*, Seita.6G148100. This gene was highly down-regulated and accumulated much fewer sRNA clusters in the 30% and 0% treatments (Fig. 8a). The *WALL-ASSOCIATED RECEPTOR KINASE-LIKE*, Seita.8G241700, showed a similar pattern of positive correlation between sRNA and mRNA expression, and the sRNA clusters mapped mostly on the exons (Fig. 8b). The *BOWMAN-BIRK INHIBITOR PROTEASE*, Seita.7G140700, and the *GLYOXALASE I*, Seita.6G036000, are examples of genes with sRNA clusters mapped in TEs inserted upstream of the transcription start site, for which the accumulation of sRNAs on those TEs negatively correlates with their mRNA expression profiles (Fig. 8c–d). In both cases, there was a reduction in TE-related sRNA accumulation and an increase in mRNA accumulation upon 30% and 0% water stress treatments. Finally, 12 of the 27 DEGs in the water deficit signaling pathway (Fig. 3) were also shown to be sRDALs (Supplementary Table 7). Among them, WRKY 18/40/60 homologs showed a positive correlation between expression and gene body sRNA accumulation, being strikingly down-regulated in both RNA-seq and sRNA-seq experiments for 30% and 0% treatment plants (Supplementary Fig. 6).

Discussion

Water deficit triggered phenotypic plasticity

Drought-tolerant plants can overcome low water availability using different strategies, depending on the stress intensity. These strategies can vary from transient phenotypic changes when submitted to low soil moisture levels to profound metabolic modulations in response to severe water stress (Basu et al. 2016; Laxa et al. 2019). Drought-tolerant C4 monocots are considered under moderate water deficit when the RWC achieves 85–96%, while plants with RWC between 80 and 85% are considered severely stressed (Carmo-Silva et al. 2008). These values are in accordance with our RWC results, allowing us to ascertain that the plants submitted to the 30% and 5–0% treatments, which showed 88% and 84% RWCs 38 days after the beginning of water deficit treatments, were cultivated under moderate and severe stress, respectively. However, the 60% treatment applied here, which showed 91% RWC, was not restrictive enough to promote physiological responses compared to the 100% treatment.

The moderate (30%) and severe (5% and 0%) water deficit treatments led to an accumulative reduction in the vegetative and reproductive growth parameters (Fig. 1; Table 1). Growth impairments in drought conditions have already been reported for several monocots, including *S. italica* (Rajala et al. 2011; Aslam et al. 2015; Luo et al. 2018; Nematpour et al. 2019). The diminishment of shoot growth, leaf size and number was associated with a lower transpiration rate under drought conditions (Blum 2005; Basu et al. 2016), which is in accordance with our results (Fig. 1).

Although plants of the 30% treatment were able to complete their lifespan, they took 24 days longer to flower and had a significant reduction in seed weight and number (Table 1). A delay in panicle emergence has been previously reported in *S. italica* under reduced irrigation conditions (Seghatoleslami et al. 2008). Late flowering can be a result of metabolism shrinkage (Cho et al. 2017) under prolonged water deficit. This result contrasts with well-known pattern of premature flowering under terminal drought (Shavrukov et al. 2017). The decrease in leaf area and seed number has been considered an adaptive strategy, ensuring reproduction under water stress conditions (Tardieu et al. 2014; Kazan and Lyons 2016). Yet, *S. italica* plants subjected to severe stress (5% and 0%) treatments prematurely perished, before flowering. After 38 days of stress treatment, we observed a marked decrease in stomatal conductance for 5% and 0% plants, which was accompanied by a reduction in the photosynthetic rate (Supplementary Table 2). Limited carbon uptake, as a result of stomatal closure, results in a decline in carbon-driven metabolism and hydraulic repair, which can ultimately promotes mortality (McDowell et al. 2018). In this context, our results suggest that one of the factors that led to the premature mortality of *S. italica* plants under severe stress was the persistent reduced CO_2 availability. Lethal drought assessment is a difficult parameter to identify, as it depends on several factors, such as drought duration and intensity (Hartmann et al. 2013). In this work, *Setaria italica* plants showed similar growth rates under the five watering regimes during the first 24 days of treatment (Fig. 1); however, as SWC decreased (Supplementary Fig. 1), plants under severe treatments perished, indicating that the water regime applied to the 5% and 0% treatments can be considered a lethal drought assessment for *S. italica*.

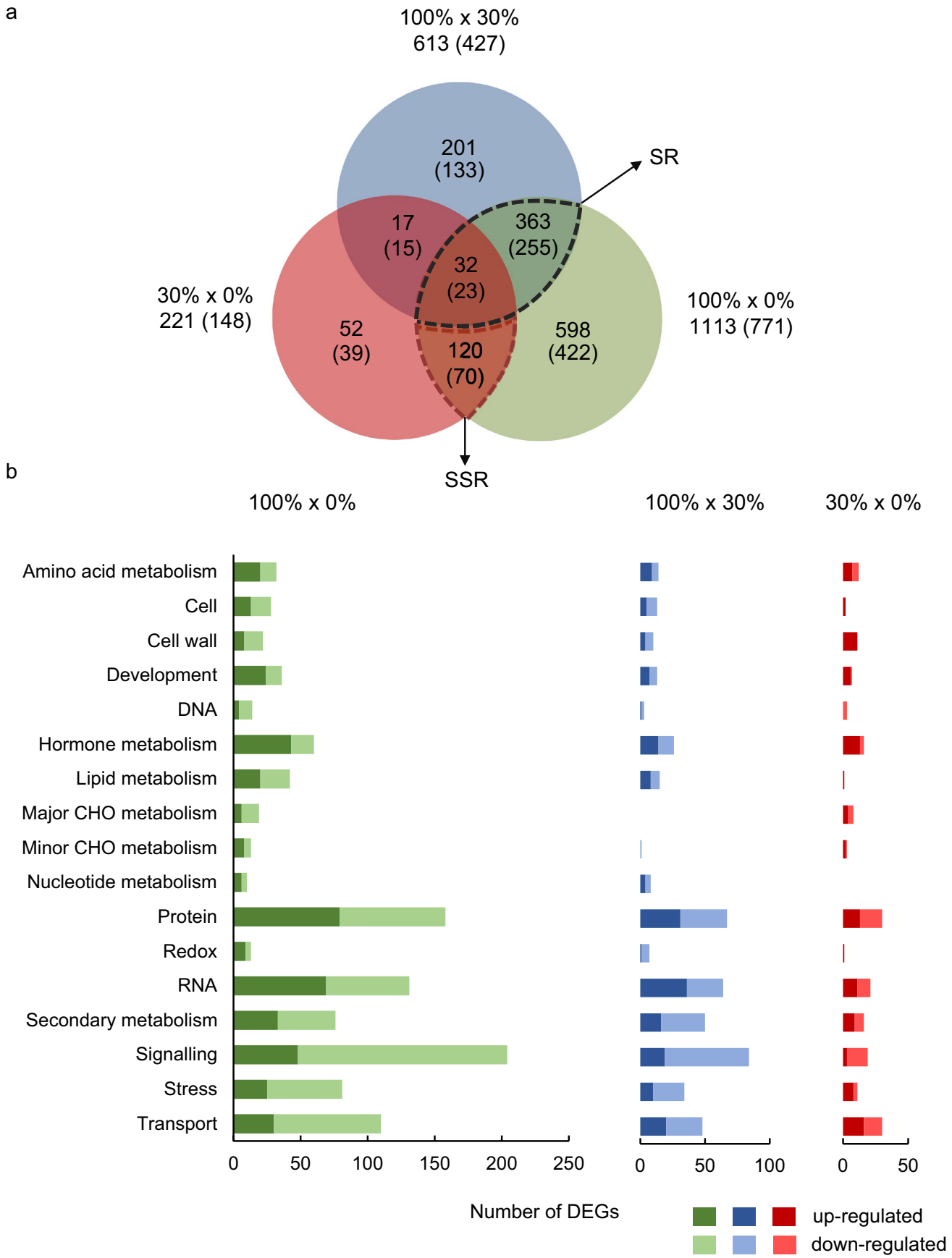
a
100% x 30%
613 (427)
201
(133)
SR
17
(15)
363
(255)
32
(23)
30% x 0%
221 (148)
52
(39)
120
(70)
598
(422)
100% x 0%
1113 (771)
SSR
b
100% x 0%
100% x 30%
30% x 0%
Amino acid metabolism
Cell
Cell wall
Development
DNA
Hormone metabolism
Lipid metabolism
Major CHO metabolism
Minor CHO metabolism
Nucleotide metabolism
Protein
Redox
RNA
Secondary metabolism
Signalling
Stress
Transport
0
50
100
150
200
250
0
50
100
0
50
Number of DEGs
up-regulated
down-regulated

◂**Fig. 2** Gene expression modulation in response to water deficit in *S. italica* leaves. **a** Venn diagram representing the distribution of DEGs that met the criteria of FDR-adjusted $P \leq 0.05$ and $\log_2$-ratio ≤ -1.0 or ≥ 1.0. The number of DEGs mapped with the MapMan tool is indicated between parentheses. SR stress-related and SSR severe stress-related DEGs are indicated by the black and red dashed lines, respectively. **b** Functional categorization of DEGs according to the main BINs of the MapMan tool. Only categories representing at least 1% of the mappings are shown. DEGs mapped to more than one category

Gene expression modulation and water deficit response

Because plasticity of morphological, developmental, and physiological phenotypes has been largely attributed to gene expression modulation, we surveyed the mRNA expression profiles of plants from 100%, 30% and 0% treatments. RNA-seq results allowed us to identify almost two thousand DEGs, and in accordance with the plant performance results, we showed a higher number of DEGs for the 100% × 0% comparison, followed by the 100% × 30% and 30% × 0% comparisons (Fig. 2a). Functional gene categorization revealed an important enrichment in categories such as signaling, protein, RNA, transport, stress, and secondary metabolism (Fig. 2b). RNA-seq was performed using leaves harvested 38 days after water stress imposition, when SWC was close to zero to 0% treatment (Supplementary Fig. 1), but plants did not have important differences in yield parameters yet (Fig. 1). Our experimental design may have favored the identification of DEGs involved in recognizing and triggering the water stress response, as previously reported for rice (Lin et al. 2017) and grapevine (Upadhyay et al. 2018) for biotic and salt stress, respectively. Our results reinforce that early stress response gene identification can be a relevant approach to studies focusing on the regulation of plant-environment interactions, including water stress.

Drought triggers complex regulatory networks, including phosphorylation signal cascades, which activate downstream regulators and effectors, and, ultimately, promote physiological adjustments in plant tissues (Takahashi et al. 2018). Foliar endogenous ABA signaling has a central role in the plant drought response, regulating stomatal closure, gene expression, and the accumulation of osmoprotective molecules (Kim et al. 2011; Zhang et al. 2018). The identification of two up-regulated *NCED* loci in water deficit treatments (Fig. 3), which catalyze the first committed step in ABA biosynthesis (Xiong and Zhu 2003), as well as an enrichment of up-regulated genes in ABA biosynthetic and signaling pathways (Fig. 4; Supplementary Table 6) reinforces the elicitor role of ABA in the *S. italica* water deficit response (Tang et al. 2017).

In the 30% and 0% treatments, DEGs that putatively encode proteins from the ABA-PYR/PYL/RCAR-PP2C-SnRK2 module, MAPK, and calcium-dependent drought-related signaling pathways were identified (Fig. 3). These signaling cascades have been involved in plant the cell response to drought stress in several plant species (Takahashi et al. 2018), including *S. italica* and its sibling species *S. viridis* (Tang et al. 2017; Duarte et al. 2019; Qin et al. 2020). Several known downstream effector-encoding genes were also differentially expressed, including putative *RBOHD*, *SLAC1*, *WRKY* and *ABF* genes. AtRBOHD belongs to a protein family responsible for the primary production of superoxide radicals in ROS signaling (Miller et al. 2009). AtSLAC1 protein regulates anion efflux to mediate stomatal closure (Vahisalu et al. 2008). The transcription factor ABF3 triggers drought-mediated chlorophyll catabolism and senescence (Hwang et al. 2019). DREB2A protein performs crosstalk between drought and heat stress signaling (Qin et al. 2008), and WRKY18/40/60 proteins are negative regulators of ABA-inducible genes, including ABFs and DREB2A (Chen et al. 2010; Shang et al. 2010). Thus, our results reinforce that the drought response triggers the canonical ABA signaling pathway in *S. italica.*

We identified two robust and stringent water deficit-responsive sets of genes, SR and SSR (Fig. 2a), which represent genes differentially expressed in both mild (30%) and intense (0%) stress conditions and genes differentially expressed only in an intense stress condition, respectively. There was a higher number of SR than SSR genes (Fig. 4), indicating that 30% and 0% plant treatments have more similarities than differences regarding the gene expression modulation in response to water deficit. The functional annotation of SR and SSR DEGs revealed that the *S. italica* response to drought involved modulation of several hormonal and signaling pathways in leaves, including an antagonistic response between ABA and auxin pathways, and AP2/EREBP and WRKY/MYB transcription factors (Fig. 4), in accordance with the literature (Asghar et al. 2019). SR and SSR genes also showed modulation of secondary metabolism pathways, mainly related to the flavonoid pathway (BIN 16.8, Supplementary Table 6). Activation of non-enzymatic antioxidant systems in RWCs from 80 to 95% was also observed in the resurrection plant *Barbacenia purpurea* (Suguiyama et al. 2014). Finally, the protein degradation pathway, especially Ubiquitin.E3 (BIN 29.5.11), was also enriched in SR and SSR genes. Ubiquitin ligase (E3) proteins participate in protein degradation by the ubiquitin (Ub)-mediated regulation pathway, which plays a role in several cellular processes, including the regulation of the water stress response (Jia et al. 2015). Taken together, our transcriptome results allowed us to catalogue several *S. italica* genes related to signaling and metabolic adjustments in response to water deficit.

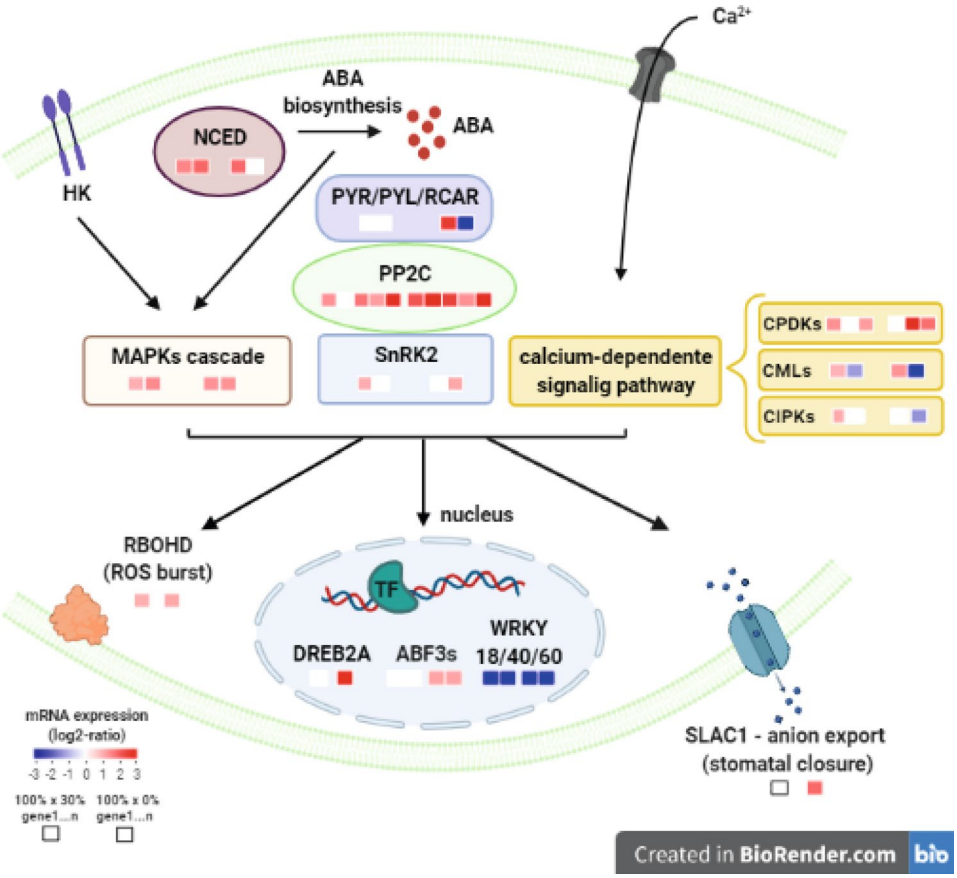

Fig. 3 *Setaria italica* signaling pathway in response to water deficit. ABA biosynthesis, HISTIDINE KINASE (HK) osmosensors and $Ca2^{+}$ transport into the cytosolic space trigger upstream regulators of the water deficit response: the PYR/PYL/RCAR-PP2C-SnRK2 module, MAPK and calcium-dependent kinase pathways (Takahashi et al. 2018). CPDKs, CIPKs and CMLs are Ca2 + -binding proteins capable of responding to or decoding dehydration signals. These pathways activate dehydration and/or ABA signaling networks by phosphorylating downstream effectors, such as anion channels, ROS-related proteins, and transcription factors. Heatmaps indicate the differential expression log2-ratio values for the 100% × 30% (squares on the left side of the protein name) and 100% × 0% (squares on the right side of the protein name) comparisons. The number of squares corresponds to the number of homologues identified. The above-mentioned genes were not differentially expressed between the 30% and 0% treatments

Setaria italica water stress-responsive genes can be regulated by sRNAs

It has been shown that stress-responsive genes are regulated at both the transcriptional and posttranscriptional levels by RNAi mechanisms (Chang et al. 2020). To obtain an overview of the *S. italica* sRNA expression profile under water deficit, we sequenced sRNA-seq libraries from 100%, 30% and 0% treatment leaves and mapped them against *S. italica* gene regulatory and body regions, as well as TEs. In accordance with DEG functional categorization, sRDALs were enriched in regulatory pathways such as protein, RNA and signaling (Figs. 2, 6), indicating that the RNAi mechanism is part of *S. italica* response to water deficit.

Plant canonical and noncanonical RdDM pathways involve siRNA biogenesis and siRNA-guided de novo DNA methylation in all sequence contexts (CG, CHG, and CHH). While 24 nt siRNAs are specifically involved in the canonical RdDM pathway and transcriptional silencing, 21–22 nt siRNAs participate in both posttranscriptional silencing and noncanonical RdDM mechanisms (Cuerda-Gil and Slotkin 2016; Wu et al. 2020). Our sRNA mapping profile showed that 24 nt sRNAs are the most abundant in the regulatory and TE regions (Fig. 5), which can be associated with canonical RdDM gene silencing. On the other hand, in the gene body regions, 21–22 nt sRNAs were preferentially mapped, suggesting that both TGS and PTGS mechanisms are important for *S. italica* gene expression modulation in response to water deficit.

siRNA-mediated epigenetic modifications are preferentially activated in the presence of TEs and other repeats (Lisch 2009), which can modulate the expression of source, homologous and neighbor loci by RdDM (Li et al. 2015). In

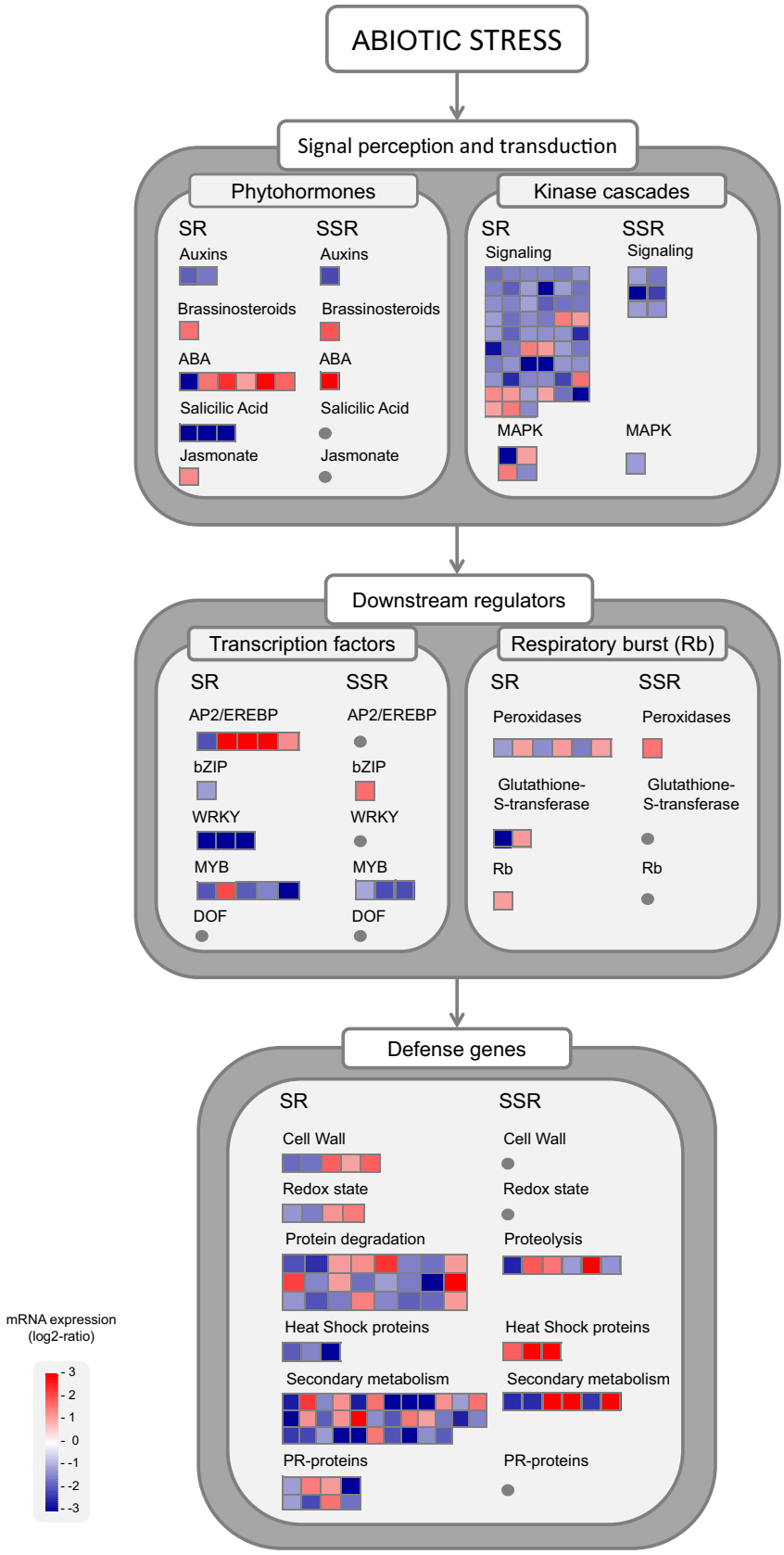

Fig. 4 Functional categorization of stress-related (SR) and severe stress-related (SSR) DEGs according to MapMan stress-related BINs. The colored boxes indicate the transcription levels of the DEGs. The gray circles indicate that no DEG was mapped in the corresponding category. The list of transcripts and the corresponding associated MapMan BINs terms are provided in Supplementary Table 6

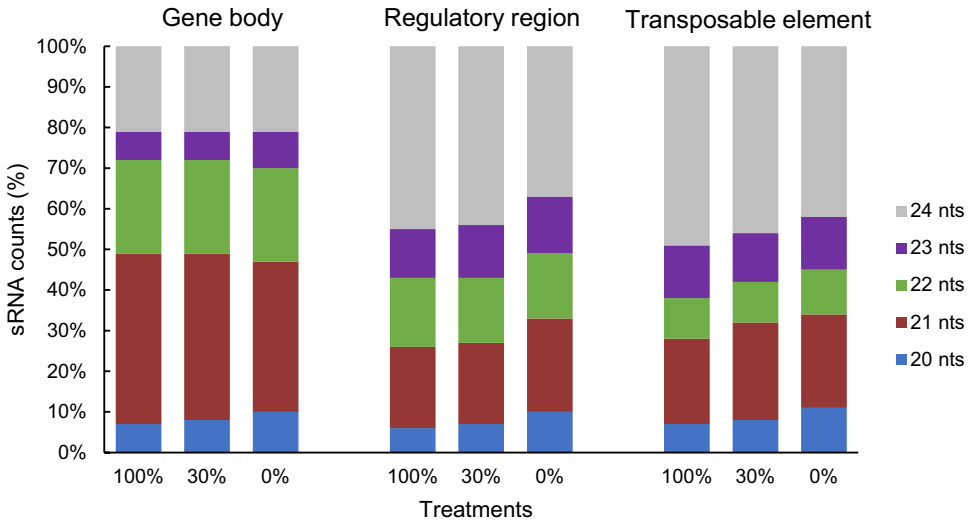

Fig. 5 sRNAs have different mapping profiles depending on the genome context. Percentage of 20–24 nt sRNAs mapped to the gene body region, regulatory region, and TE insertions for the 100%, 30% and 0% treatments

this sense, we were able to identify 14 and six DEGs with differential accumulation of sRNAs in TEs inserted in their regulatory and gene body regions, respectively. All 20 genes were SR DEGs; however, they had different expression profiles of mRNA and sRNA (Supplementary Table 11) and were annotated to various MapMan functional categories (Supplementary Table 6). At least five of these loci code for proteins that had homologous pairs participating in abiotic stress response, as follows: a *GLYOXALASE I* protein, which prevents oxidative damage during abiotic stress episodes by methylglyoxal detoxification (Batth et al. 2020); a serine protease BOWMAN-BIRK INHIBITOR PROTEASE (Yan et al. 2009; Malefo et al. 2020); a CALRETICULIN 3 protein that plays a role on Ca^{2+}-dependent processes during water stress response (Kim et al. 2011); a MOLYBDATE TRANSPORTER 2, responsible for molybdate transfer from leaves to seeds during plant senescence (Gasber et al. 2011) and the NAC transcription factor ATAF2, which induces early leaf senescence (Nagahage et al. 2020). The coordinated mRNA and sRNA differential expression of these genes improves our knowledge of the water deficit responses in the drought-tolerant grass *S. italica*, suggesting that at least in part, TEs in the *S. italica* genome are involved in RdDM gene expression modulation.

Due to the nature of gene expression silencing mechanisms, a negative correlation between mRNA and sRNA expression levels is expected for genes regulated by the RNAi mechanism. Although we identified several DEGs negatively correlated with sRDALs, we found no global correlation between SR and SSR DEGs and sRDALs in the regulatory regions, while a positive correlation was observed in the gene body regions (Fig. 5). Hypermethylation of gene bodies was positively correlated with high gene expression levels in maize and *A. thaliana* plants (Zhang et al. 2006; Li et al. 2015; Lu et al. 2015); however, the mechanism underlying this pattern is poorly understood. Chaudhary and colleagues hypothesized that under stress conditions, plants buffer against normal protein synthesis via alternative splicing coupled to decreased RNA decay to produce protein variants responsible for adaptation to stress. This strategy could reduce stress metabolic cost and include stress-responsive alternative isoforms in the proteome (Chaudhary et al. 2019). RNA decay is a cytoplasmic mRNA quality control mechanism that targets newly synthesized transcripts for degradation by exonucleases, antagonizing or circumventing the mechanisms that initiate the RNAi pathway by either generating or removing template RNA molecules that could be used by PTGS or RdDM (Crisp et al. 2016). On the other hand, a massive accumulation of 22 nt siRNAs has been reported in plants deficient in both PTGS and RNA decay mechanisms under abiotic stress, including activation of stress signaling and repression of growth loci (Wu et al. 2020). Although much remains to be elucidated about the gene expression regulation associated with sRNAs mapping to gene bodies, our results reinforce that TGS and PTGS are important for *S. italica* water deficit response regulation and pinpoint that sRNA homologous to gene body regions might have an important role in that response, which should be better understood to untangle the intricate and multimechanistic pathways involved in gene expression modulation in the monocot drought response.

Conclusion

The experiments submitting *S. italica* plants to five watering regimes performed in this study allowed the broadening of the knowledge about the adaptive strategies adopted

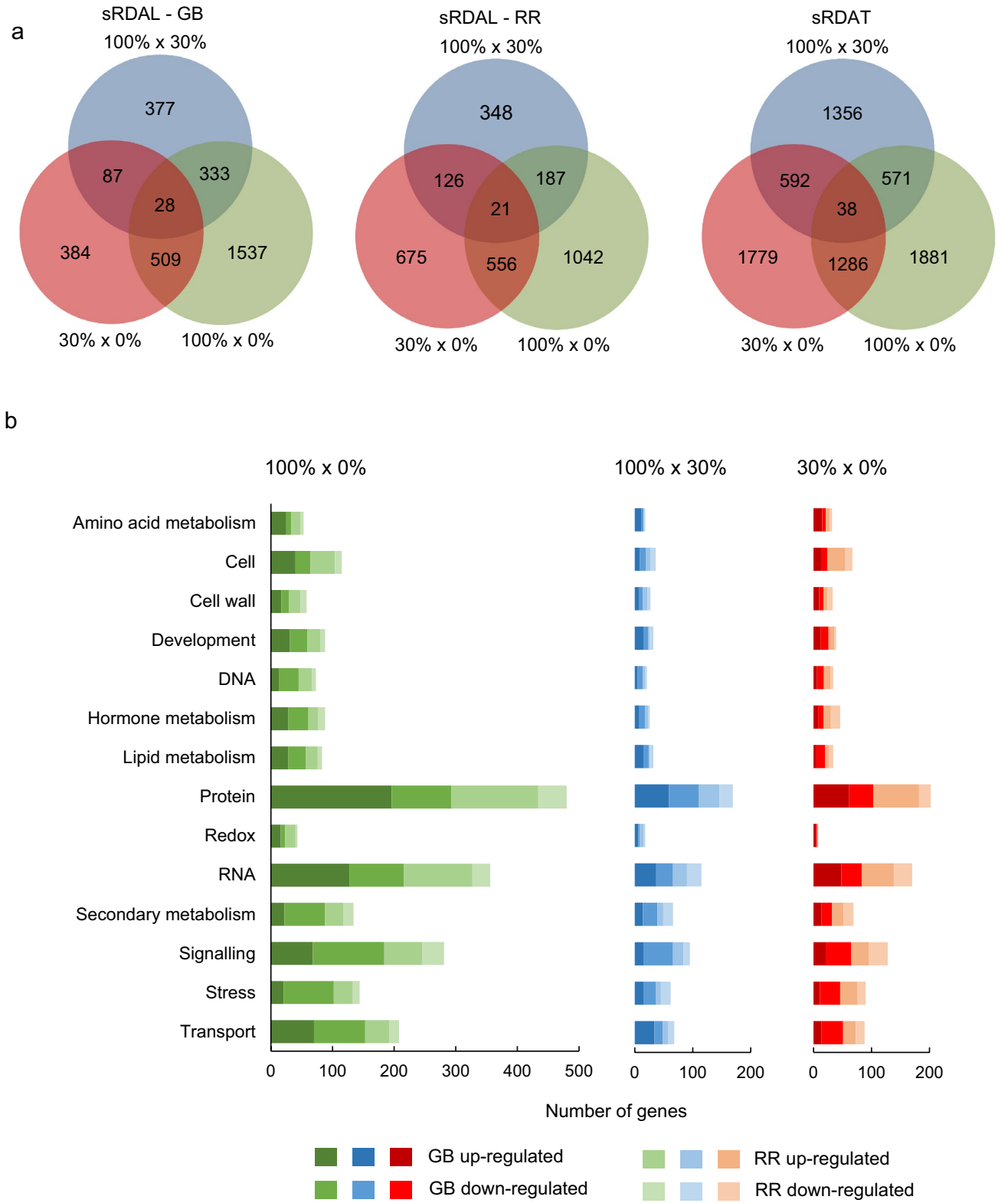

Fig. 6 sRNA expression modulation in response to water deficit in *S. italica* leaves. **a** Venn diagram representing the distribution of sRDALs mapped against gene body (GB) and regulatory (RR) regions, and sRNA differentially accumulated on TE sequences (sRDATs) in the three treatment comparisons. **b** Functional categorization of sRDAL-mapped genes according to the main BINs of the MapMan tool. Only categories representing at least 1% of the mappings in the comparison are shown. DEGs mapped to more than one category

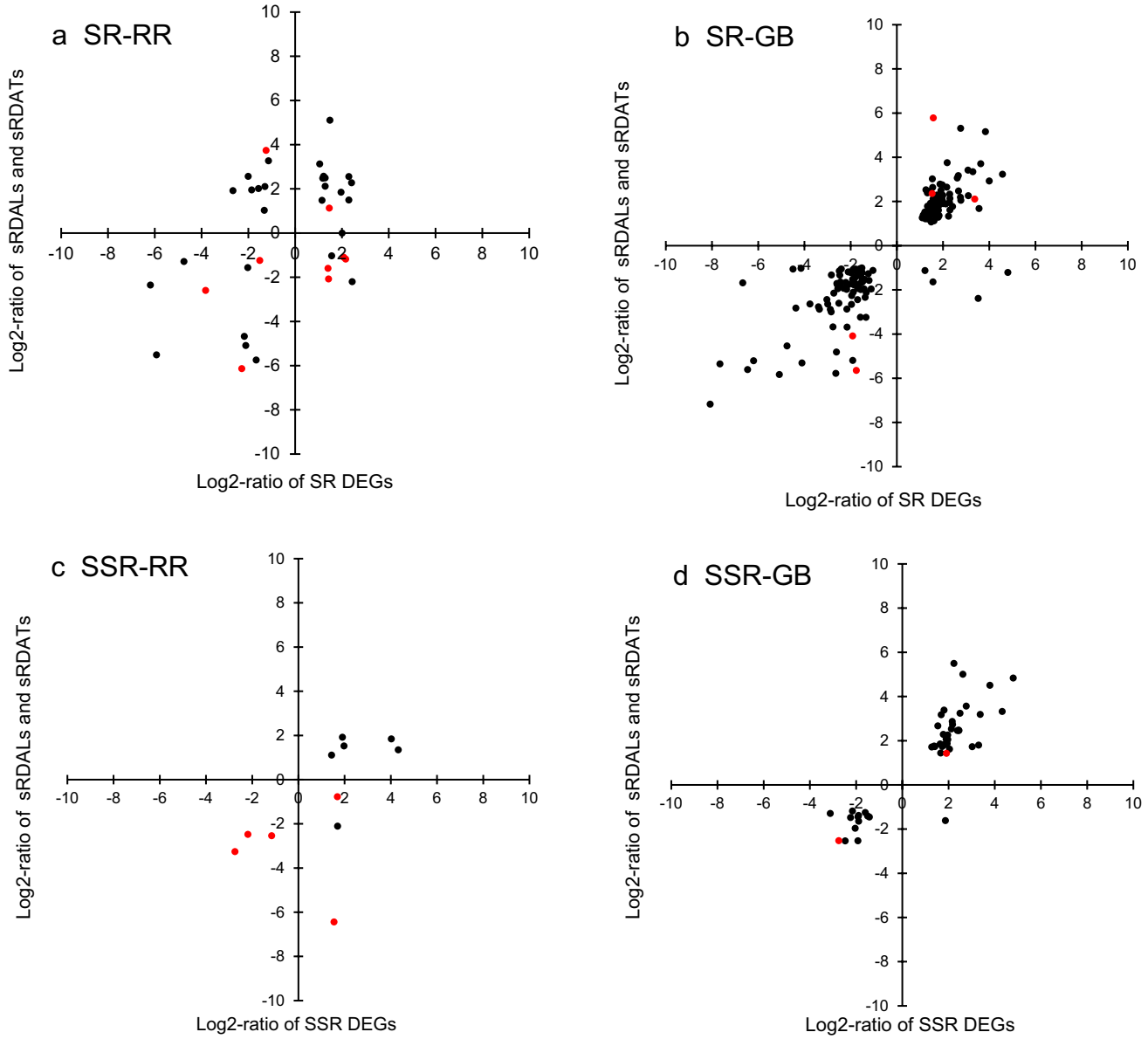

Fig. 7 Correlation analyses between gene expression and sRDAL (black dots) / sRDAT (red dots) profiles for regulatory regions of SR DEGs (**a**, Spearman correlation, R = 0.36, P > 0.01), gene body regions of SR DEGs (**b**, Spearman correlation, R = 0.84, P < 0.01), regulatory regions of SSR DEGs (**c**, Spearman correlation, R = 0.76, P > 0.01) and, gene body regions of SSR DEGs (**d**, Spearman correlation, R = 0.79, P < 0.01)

by this species to the selective pressure imposed by water stress. The analysis of vegetative and reproductive growth, physiological, and genetic parameters showed that *S. italica* differentially responded to distinct water stress intensities. Additionally, we were able to catalogue several candidate genes related to water stress signaling and metabolic adjustments, which seems to have a role in *S. italica* phenotypic plasticity. Furthermore, our results indicated that sRNA-dependent gene expression regulation mechanisms contribute to the *S. italica* water deficit responses, providing an adaptive epigenetic line of defense against drought.

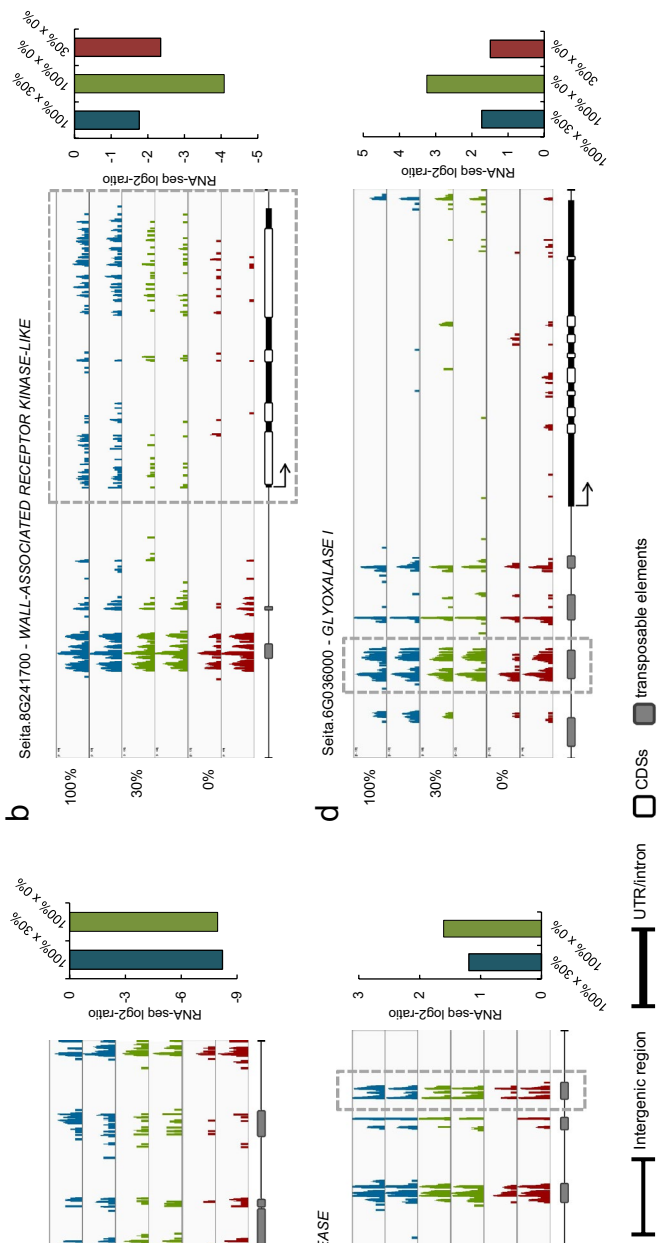

Fig. 8 sRDAL profiles evidence gene expression modulation in response to water deficit. Seita.6G148100 (**a**) and Seita.8G241700 (**b**) exemplify the positive correlation between gene expression and gene body small RNA mapping under water deficit. These loci were downregulated in both RNA-seq and sRNA-seq experiments for the 30% and 0% treatments. Seita.7G140700 (**c**) and Seita.6G036000 (**d**) loci were up-regulated in the RNA-seq experiment for the 30% and 0% treatments and showed a down-accumulation of sRDALs in TEs inserted in the 5' regulatory regions. Tracks show the mapping position of sRNA reads for 100% (blue), 30% (green) and 0% (red) treatments. Dotted gray frames indicate sRDAL regions. Histograms show the log2-ratio of DEGs

Supplementary Information The online version contains supplementary material available at https://doi.org/10.1007/s11103-022-01273-w.

Acknowledgements We thank Dr Hugo Bruno Correa Mollinari for providing us with the seeds of *S. italica* YUGU1.

Author contributions Conceptualization: VFS, ELB, DCC, MR and NS; RNA-seq analysis: VFS, LAH, NB, FC, LFB, and NS; Yield and physiological analysis: VFS, JDPR, TCNS, JPNS, EAS and DC; Carbohydrate quantification: VFS, BSL and EP; RT-pPCR validation: VFS and BSL; Formal analysis: VFS and NS; Writing-original draft preparation: VFS, MR and NS; Writing-review and editing: all authors.

Funding Fundação de Amparo à Pesquisa do Estado de São Paulo (FAPESP), Grant Numbers: 2012/23838–7 to DCC and 2015/16975–6 to NS. Coordenação de Aperfeiçoamento de Pessoal de Ensino Superior (CAPES), Scholarship to VFS and JDPR.

Data availability The data that support the findings of this study are openly available in NCBI Bioproject at https://www.ncbi.nlm.nih.gov/bioproject, reference number PRJNA593563.

Declarations

Conflict of interest The authors have no relevant financial or non-financial interests to disclose.

References

Anders S, Pyl PT, Huber W (2015) HTSeq-A Python framework to work with high-throughput sequencing data. Bioinformatics 31:166–169. https://doi.org/10.1093/bioinformatics/btu638

Asghar MA, Li Y, Jiang H, Sun X, Ahmad B, Imran S, Yu L, Liu C, Yang W, Du J (2019) Crosstalk between abscisic acid and auxin under osmotic stress. Agron J 111:2157–2162. https://doi.org/10.2134/agronj2018.10.0633

Aslam M, Zamir MSI, Anjum SA, Khan I, Tanveer M (2015) An investigation into morphological and physiological approaches to screen maize (Zea mays L.) hybrids for drought tolerance. Cereal Res Commun 43:41–51. https://doi.org/10.1556/CRC.2014.0022

Axtell MJ (2013) ShortStack: comprehensive annotation and quantification of small RNA genes. RNA 19:740–751. https://doi.org/10.1261/rna.035279.112

Basu S, Ramegowda V, Kumar A, Pereira A (2016) Plant adaptation to drought stress. F1000Research 5:1554

Batth R, Jain M, Kumar A, Nagar P, Kumari S, Mustafiz A (2020) Zn^{2+} dependent glyoxalase i plays the major role in methylglyoxal detoxification and salinity stress tolerance in plants. PLoS One 15:1–14. https://doi.org/10.1371/journal.pone.0233493

Bennetzen JL, Schmutz J, Wang H, Percifield R, Hawkins J, Pontaroli AC, Estep M, Feng L, Vaughn JN, Grimwood J, Jenkins J, Barry K, Lindquist E, Hellsten U, Deshpande S, Wang X, Wu X, Mitros T, Triplett J, Yang X, Ye CY, Mauro-Herrera M, Wang L, Li P, Sharma M, Sharma R, Ronald PC, Panaud O, Kellogg EA, Brutnell TP, Doust AN, Tuskan GA, Rokhsar D, Devos KM (2012) Reference genome sequence of the model plant Setaria. Nat Biotechnol 30:555–561. https://doi.org/10.1038/nbt.2196

Blum A (2005) Drought resistance, water-use efficiency, and yield potential are they compatible, dissonant, or mutually exclusive? Aust J Agric Res 56:1159–1168. https://doi.org/10.1071/AR05069

Bolger AM, Lohse M, Usadel B (2014) Genome analysis Trimmomatic: a flexible trimmer for Illumina sequence data. Bioinformatics 30:2114–2120. https://doi.org/10.1093/bioinformatics/btu170

Brkljacic J, Grotewold E (2017) Combinatorial control of plant gene expression. Biochim Biophys Acta 1860:31–40. https://doi.org/10.1016/j.bbagrm.2016.07.005

Carmo-Silva AE, Powers SJ, Keys AJ, Arrabaça MC, Parry MAJ (2008) Photorespiration in C4 grasses remains slow under drought conditions. Plant, Cell Environ 31:925–940. https://doi.org/10.1111/j.1365-3040.2008.01805.x

Chang YN, Zhu C, Jiang J, Zhang H, Zhu JK, Duan CG (2020) Epigenetic regulation in plant abiotic stress responses. J Integr Plant Biol 62:563–580. https://doi.org/10.1111/jipb.12901

Chaudhary S, Jabre I, Reddy ASN, Staiger D, Syed NH (2019) Perspective on alternative splicing and proteome complexity in plants. Trends Plant Sci 24:496–506. https://doi.org/10.1016/j.tplants.2019.02.006

Chaves MM, Maroco JP, Pereira JS (2003) Understanding plant responses to drought from genes to the whole plant. Funct Plant Biol 30:239–264. https://doi.org/10.1071/FP02076

Chen H, Lai Z, Shi J, Xiao Y, Chen Z, Xu X (2010) Roles of arabidopsis WRKY18, WRKY40 and WRKY60 transcription factors in plant responses to abscisic acid and abiotic stress. BMC Plant Biol 10:281. https://doi.org/10.1186/1471-2229-10-281

Cho LH, Yoon J, An G (2017) The control of flowering time by environmental factors. Plant J 90:708–719. https://doi.org/10.1111/tpj.13461

Crisp PA, Ganguly D, Eichten SR, Borevitz JO, Pogson BJ (2016) Reconsidering plant memory: intersections between stress recovery, RNA turnover, and epigenetics. Sci Adv 2:e1501340. https://doi.org/10.1126/sciadv.1501340

Cuerda-Gil D, Slotkin RK (2016) Non-canonical RNA-directed DNA methylation. Nat Plants 2:16211. https://doi.org/10.1038/nplants.2016.163

Doust AN, Kellogg EA, Devos KM, Bennetzen JL (2009) Foxtail millet: a sequence-driven grass model system. Plant Physiol 149:137–141. https://doi.org/10.1104/pp.108.129627

Duarte KE, de Souza WR, Santiago TR, Sampaio BL, Ribeiro AP, Cotta MG, da Cunha BADB, Marraccini PRR, Kobayashi AK, Molinari HBC (2019) Identification and characterization of core abscisic acid (ABA) signaling components and their gene expression profile in response to abiotic stresses in Setaria viridis. Sci Rep 9:4028. https://doi.org/10.1038/s41598-019-40623-5

Fracasso A, Trindade LM, Amaducci S (2016) Drought stress tolerance strategies revealed by RNA-Seq in two sorghum genotypes with contrasting WUE. BMC Plant Biol 16:115. https://doi.org/10.1186/s12870-016-0800-x

Gasber A, Klaumann S, Trentmann O, Trampczynska A, Clemens S, Schneider S, Sauer N, Feifer I, Bittner F, Mendel RR, Neuhaus HE (2011) Identification of an Arabidopsis solute carrier critical for intracellular transport and inter-organ allocation of molybdate. Plant Biol 13:710–718. https://doi.org/10.1111/j.1438-8677.2011.00448.x

Gentleman RC, Carey VJ, Bates DM, Bolstad B, Dettling M, Dudoit S, Ellis B, Gautier L, Ge Y, Gentry J, Hornik K, Hothorn T, Huber W, Iacus S, Irizarry R, Leisch F, Li C, Maechler M, Rossini AJ, Sawitzki G, Smith C, Smyth G, Tierney L, Yang JYH, Zhang J (2004) Bioconductor: open software development for computational biology and bioinformatics. Genome Biol 5:R80. https://doi.org/10.1186/gb-2004-5-10-r80

Hammer Ø, Harper DA, Ryan PD (2001) Past: paleontological statistics software package for education and data analysis. Palaeontol Electron 4:1–9

Hartmann H, Ziegler W, Trumbore S (2013) Lethal drought leads to reduction in nonstructural carbohydrates in Norway spruce tree

roots but not in the canopy. Funct Ecol 27:413–427. https://doi.org/10.1111/1365-2435.12046
Hoang XLT, Nhi DNH, Thu NBA, Thao NP, Tran L-SP (2017) Transcription factors and their roles in signal transduction in plants under abiotic stresses. Curr Genomics 18:483–497. https://doi.org/10.2174/1389202918666170227150057
Hung Y-H, Slotkin RK (2021) The initiation of RNA interference (RNAi) in plants. Curr Opin Plant Biol 61:102014. https://doi.org/10.1016/j.pbi.2021.102014
Hwang K, Susila H, Nasim Z, Jung J-Y, Ahn JH (2019) Arabidopsis ABF3 and ABF4 transcription factors act with the NF-YC complex to regulate SOC1 expression and mediate drought-accelerated flowering. Mol Plant 12:489–505. https://doi.org/10.1016/j.molp.2019.01.002
Jia F, Wang C, Huang J, Yang G, Wu C, Zheng C (2015) SCF E3 ligase PP2-B11 plays a positive role in response to salt stress in Arabidopsis. J Exp Bot 66:4683–4697. https://doi.org/10.1093/jxb/erv245
Kang D-J, Futakuchi K (2019) Effect of moderate drought-stress on flowering time of interspecific hybrid progenies (Oryza sativa L. × Oryza glaberrima Steud.). J Crop Sci Biotechnol 22:75–81. https://doi.org/10.1007/s12892-019-0015-0
Kazan K, Lyons R (2016) The link between flowering time and stress tolerance. J Exp Bot 67:47–60. https://doi.org/10.1093/jxb/erv441
Kim J-S, Mizoi J, Yoshida T, Fujita Y, Nakajima J, Ohori T, Todaka D, Nakashima K, Hirayama T, Shinozaki K, Yamaguchi-Shinozaki K (2011) An ABRE promoter sequence is involved in osmotic stress-responsive expression of the DREB2A gene, which encodes a transcription factor regulating drought-inducible genes in Arabidopsis. Plant Cell Physiol 52:2136–2146. https://doi.org/10.1093/pcp/pcr143
Konopka-Postupolska D, Dobrowolska G (2020) ABA perception is modulated by membrane receptor-like kinases. J Exp Bot 71:1210–1214. https://doi.org/10.1093/jxb/erz531
Lambret-Frotté J, De Almeida LCS, De Moura SM, Souza FLF, Linhares FS, Alves-Ferreira M (2015) Validating internal control genes for the accurate normalization of qPCR expression analysis of the novel model plant Setaria viridis. PLoS ONE 10:e0135006. https://doi.org/10.1371/journal.pone.0135006
Lata C, Sahu PP, Prasad M (2010) Comparative transcriptome analysis of differentially expressed genes in foxtail millet (Setaria italica L.) during dehydration stress. Biochem Biophys Res Commun 393:720–727. https://doi.org/10.1016/j.bbrc.2010.02.068
Laxa M, Liebthal M, Telman W, Chibani K, Dietz K-J (2019) The role of the plant antioxidant system in drought tolerance. Antioxidants 8:94. https://doi.org/10.3390/antiox8040094
Li Q, Gent JI, Zynda G, Song J, Makarevitch I, Hirsch CD, Hirsch CN, Dawe RK, Madzima TF, McGinnis KM, Lisch D, Schmitz RJ, Vaughn MW, Springer NM (2015) RNA-directed DNA methylation enforces boundaries between heterochromatin and euchromatin in the maize genome. Proc Natl Acad Sci USA 112:14728–14733. https://doi.org/10.1073/pnas.1514680112
Lin CW, Huang LY, Huang CL, Wang YC, Lai PH, Wang HV, Chang WC, Chiang TY, Huang HJ (2017) Common stress transcriptome analysis reveals functional and genomic architecture differences between early and delayed response genes. Plant Cell Physiol 58:546–559. https://doi.org/10.1093/pcp/pcx002
Lisch D (2009) Epigenetic regulation of transposable elements in plants. Annu Rev Plant Biol 60:43–66. https://doi.org/10.1146/annurev.arplant.59.032607.092744
Liu W, Stewart CN (2016) Plant synthetic promoters and transcription factors. Curr Opin Biotechnol 37:36–44. https://doi.org/10.1016/j.copbio.2015.10.001
Lohse M, Nagel A, Herter T, May P, Schroda M, Zrenner R, Tohge T, Fernie AR, Stitt M, Usadel B (2014) Mercator: a fast and simple web server for genome scale functional annotation of plant sequence data. Plant, Cell Environ 37:1250–1258. https://doi.org/10.1111/pce.12231
Love MI, Huber W, Anders S (2014) Moderated estimation of fold change and dispersion for RNA-seq data with DESeq2. Genome Biol 15:550. https://doi.org/10.1186/s13059-014-0550-8
Lu X, Wang W, Ren W, Chai Z, Guo W, Chen R, Wang L, Zhao J, Lang Z, Fan Y, Zhao J, Zhang C (2015) Genome-wide epigenetic regulation of gene transcription in maize seeds. PLoS ONE 10:e0139582. https://doi.org/10.1371/journal.pone.0139582
Luo F, Deng X, Liu Y, Yan Y (2018) Identification of phosphorylation proteins in response to water deficit during wheat flag leaf and grain development. Bot Stud 59:28. https://doi.org/10.1186/s40529-018-0245-7
Malefo MB, Mathibela EO, Crampton BG, Makgopa ME (2020) Investigating the role of Bowman-Birk serine protease inhibitor in Arabidopsis plants under drought stress. Plant Physiol Biochem 149:286–293. https://doi.org/10.1016/j.plaphy.2020.02.007
Matzke MA, Mosher RA (2014) RNA-directed DNA methylation: an epigenetic pathway of increasing complexity. Nat Rev Genet 15:394–408. https://doi.org/10.1038/nrg3683
McDowell N, Allen CD, Anderson-Teixeira K, Brando P, Brienen R, Chambers J, Christoffersen B, Davies S, Doughty C, Duque A, Espirito-Santo F, Fisher R, Fontes CG, Galbraith D, Goodsman D, Grossiord C, Hartmann H, Holm J, Johnson DJ, Kassim AR, Keller M, Koven C, Kueppers L, Kumagai T, Malhi Y, McMahon SM, Mencuccini M, Meir P, Moorcroft P, Muller-Landau HC, Phillips OL, Powell T, Sierra CA, Sperry J, Warren J, Xu C, Xu X (2018) Drivers and mechanisms of tree mortality in moist tropical forests. New Phytol 219:851–869. https://doi.org/10.1111/nph.15027
Miller G, Schlauch K, Tam R, Cortes D, Torres MA, Shulaev V, Dangl JL, Mittler R (2009) The plant NADPH oxidase RBOHD mediates rapid systemic signaling in response to diverse stimuli. Sci Signal. https://doi.org/10.1126/scisignal.2000448
Nagahage ISP, Sakamoto S, Nagano M, Ishikawa T, Mitsuda N, Kawai-Yamada M, Yamaguchi M (2020) An Arabidopsis NAC domain transcription factor, ATAF2, promotes age-dependent and dark-induced leaf senescence. Physiol Plant 170:299–308. https://doi.org/10.1111/ppl.13156
Nematpour A, Eshghizadeh HR, Zahedi M (2019) Drought-tolerance mechanisms in foxtail millet (Setaria italica) and proso millet (Panicum miliaceum) under different nitrogen supply and sowing dates. Crop Pasture Sci 70:442–452. https://doi.org/10.1071/CP18501
Nicotra AB, Atkin OK, Bonser SP, Davidson AM, Finnegan EJ, Mathesius U, Poot P, Purugganan MD, Richards CL, Valladares F, van Kleunen M (2010) Plant phenotypic plasticity in a changing climate. Trends Plant Sci 15:684–692. https://doi.org/10.1016/j.tplants.2010.09.008
Pfaffl MW, Horgan GW, Dempfle L (2002) Relative expression software tool (REST) for group-wise comparison and statistical analysis of relative expression results in real-time PCR. Nucleic Acids Res 30:e36. https://doi.org/10.1093/nar/30.9.e36
Qi X, Xie S, Liu Y, Yi F, Yu J (2013) Genome-wide annotation of genes and noncoding RNAs of foxtail millet in response to simulated drought stress by deep sequencing. Plant Mol Biol 83:459–473. https://doi.org/10.1007/s11103-013-0104-6
Qin F, Sakuma Y, Tran L-SP, Maruyama K, Kidokoro S, Fujita Y, Fujita M, Umezawa T, Sawano Y, Miyazono K-I, Tanokura M, Shinozaki K, Yamaguchi-Shinozaki K (2008) Arabidopsis DREB2A-interacting proteins function as RING E3 ligases and negatively regulate plant drought stress-responsive gene expression. Plant Cell 20:1693–1707. https://doi.org/10.1105/tpc.107.057380
Qin L, Chen E, Li F, Yu X, Liu Z, Yang Y, Wang R, Zhang H, Wang H, Liu B, Guan Y, Ruan Y (2020) Genome-wide gene expression profiles analysis reveal novel insights into drought stress in foxtail

millet (Setaria italica L). Int J Mol Sci 21:8520. https://doi.org/10.3390/ijms21228520
Quadrana L, Almeida J, Asís R, Duffy T, Dominguez PG, Bermúdez L, Conti G, da Silva JVC, Peralta IE, Colot V, Asurmendi S, Fernie AR, Rossi M, Carrari F (2014) Natural occurring epialleles determine vitamin E accumulation in tomato fruits. Nat Commun 5:4027. https://doi.org/10.1038/ncomms5027
Rajala A, Hakala K, Mäkelä P, Peltonen-Sainio P (2011) Drought effect on grain number and grain weight at spike and spikelet level in six-row spring barley. J Agron Crop Sci 197:103–112. https://doi.org/10.1111/j.1439-037X.2010.00449.x
Robinson MD, McCarthy DJ, Smyth GK (2010) edgeR: a Bioconductor package for differential expression analysis of digital gene expression data. Bioinformatics 26:139–140. https://doi.org/10.1093/bioinformatics/btp616
Ruijter JM, Ramakers C, Hoogaars WMH, Karlen Y, Bakker O, van den hoff MJB, Moorman AFM, (2009) Amplification efficiency: linking baseline and bias in the analysis of quantitative PCR data. Nucleic Acids Res 37:e45. https://doi.org/10.1093/nar/gkp045
Seghatoleslami MJ, Kafi M, Majidi E (2008) Effect of deficit irrigation on yield, wue and some morphological and phenological traits of three millet species. Pakistan J Bot 40:1555–1560
Shang Y, Yan L, Liu Z-Q, Cao Z, Mei C, Xin Q, Wu F-Q, Wang X-F, Du S-Y, Jiang T, Zhang X-F, Zhao R, Sun H-L, Liu R, Yu Y-T, Zhang D-P (2010) The Mg-chelatase H subunit of Arabidopsis antagonizes a group of WRKY transcription repressors to relieve ABA-responsive genes of inhibition. Plant Cell 22:1909–1935. https://doi.org/10.1105/tpc.110.073874
Shavrukov Y, Kurishbayev A, Jatayev S, Shvidchenko V, Zotova L, Koekemoer F, De Groot S, Soole K, Langridge P (2017) Early flowering as a drought escape mechanism in plants: How can it aid wheat production? Front Plant Sci 8:1950. https://doi.org/10.3389/fpls.2017.01950
Su Z, Ma X, Guo H, Sukiran NL, Guo B, Assmann SM, Ma H (2013) Flower development under drought stress: morphological and transcriptomic analyses reveal acute responses and long-term acclimation in Arabidopsis. Plant Cell 25:3785–3807. https://doi.org/10.1105/tpc.113.115428
Sudan J, Raina M, Singh R (2018) Plant epigenetic mechanisms: role in abiotic stress and their generational heritability. 3 Biotech 8:172. https://doi.org/10.1007/s13205-018-1202-6
Suguiyama VF, Silva EA, Meirelles ST, Centeno DC, Braga MR (2014) Leaf metabolite profile of the Brazilian resurrection plant Barbacenia purpurea Hook. (Velloziaceae) shows two time-dependent responses during desiccation and recovering. Front Plant Sci 5:96. https://doi.org/10.3389/fpls.2014.00096
Suguiyama VF, Vasconcelos LAB, Rossi MM, Biondo C, de Setta N (2019) The population genetic structure approach adds new insights into the evolution of plant LTR retrotransposon lineages. PLoS ONE 14:e0214542. https://doi.org/10.1371/journal.pone.0214542
Sun C, Gao X, Chen X, Fu J, Zhang Y (2016) Metabolic and growth responses of maize to successive drought and re-watering cycles. Agric Water Manag 172:62–73. https://doi.org/10.1016/j.agwat.2016.04.016
Takahashi F, Kuromori T, Sato H, Shinozaki K (2018) Regulatory gene networks in drought stress responses and resistance in plants. In: Iwaya-Inoue M, Sakurai M, Uemura M (eds) Survival Strategies in Extreme Cold and Desiccation, 1st edn. Springer, Singapore, pp 189–214
Tang S, Li L, Wang Y, Chen Q, Zhang W, Jia G, Zhi H, Zhao B, Diao X (2017) Genotype-specific physiological and transcriptomic responses to drought stress in Setaria italica (an emerging model for Panicoideae grasses). Sci Rep 7:10009. https://doi.org/10.1038/s41598-017-08854-6
Tardieu F, Parent B, Caldeira CF, Welcker C (2014) Genetic and physiological controls of growth under water deficit. Plant Physiol 164:1628–1635. https://doi.org/10.1104/pp.113.233353
Upadhyay A, Gaonkar T, Upadhyay AK, Jogaiah S, Shinde MP, Kadoo NY, Gupta VS (2018) Global transcriptome analysis of grapevine (Vitis vinifera L) leaves under salt stress reveals differential response at early and late stages of stress in table grape cv. Elsevier Masson, Les Collectionneurs
Usadel B, Poree F, Nagel A, Lohse M, Czedik-Eysenberg A, Stitt M (2009) A guide to using MapMan to visualize and compare Omics data in plants: a case study in the crop species, Maize. Plant, Cell Environ 32:1211–1229. https://doi.org/10.1111/j.1365-3040.2009.01978.x
Vahisalu T, Kollist H, Wang Y-F, Nishimura N, Chan W-Y, Valerio G, Lamminmäki A, Brosché M, Moldau H, Desikan R, Schroeder JI, Kangasjärvi J, Lamminmaki A, Brosche M, Moldau H, Desikan R, Schroeder JI, Kangasjarvi J (2008) SLAC1 is required for plant guard cell S-type anion channel. Nature 452:487–491. https://doi.org/10.1038/nature06608.SLAC1
Weatherley PE (1950) Studies in the water relations of the cotton plant. New Phytol 49:81–97
Wu TD, Reeder J, Lawrence M, Becker G, Brauer MJ (2016) GMAP and GSNAP for genomic sequence alignment: enhancements to speed, accuracy, and functionality. In: Mathé E, Davis S (eds) Statistical Genomics: Methods and Protocolos, 1st edn. Springer Science and Business Media, New York, pp 283–334
Wu H, Li B, Iwakawa H, Pan Y, Tang X, Ling-hu Q, Liu Y, Sheng S, Feng L, Zhang H, Zhang X, Tang Z, Xia X, Zhai J, Guo H (2020) Plant 22-nt siRNAs mediate translational repression and stress adaptation. Nature 581:89–93. https://doi.org/10.1038/s41586-020-2231-y
Xiong L, Zhu J-K (2003) Regulation of abscisic acid biosynthesis. Plant Physiol 133:29–36. https://doi.org/10.1104/pp.103.025395
Xu B, Li F, Shan L, Ma Y, Ichizen N, Huang J (2006) Gas exchange, biomass partition, and water relationships of three grass seedlings under water stress. Weed Biol Manag 6:79–88. https://doi.org/10.1111/j.1445-6664.2006.00197.x
Yan KM, Chang T, Soon SA, Huang FY (2009) Purification and characterization of bowman-birk protease inhibitor from rice coleoptiles. J Chinese Chem Soc 56:949–960. https://doi.org/10.1002/jccs.200900139
Zadoks JC, Chang TT, Konzak CF (1974) A decimal code for the growth stages of cereals. Weed Res 14:415–421. https://doi.org/10.1111/j.1365-3180.1974.tb01084.x
Zhang X, Yazaki J, Sundaresan A, Cokus S, Chan SW-L, Chen H, Henderson IR, Shinn P, Pellegrini M, Jacobsen SE, Ecker JRR (2006) Genome-wide high-resolution mapping and functional analysis of DNA methylation in Arabidopsis. Cell 126:1189–1201. https://doi.org/10.1016/j.cell.2006.08.003
Zhang FP, Sussmilch F, Nichols DS, Cardoso AA, Brodribb TJ, McAdam SAM (2018) Leaves, not roots or floral tissue, are the main site of rapid, external pressure-induced ABA biosynthesis in angiosperms. J Exp Bot 69:1261–1267. https://doi.org/10.1093/jxb/erx480